THE RESEARCH AND APPLICATION OF COMBINING LUT AND MEMORY COMPENSATION FOR TWTA LINEARIZATION WITH RELATIVELY LOW SAMPLING FREQUENCY

X. Hu[1, *], G. Wang[2], Q.-L. Li[2], Z.-C. Wang[2], and J.-R. Luo[2]

[1]Research & Development (R&D) Center of China Academy of Launch Vehicle Technology, Beijing, China

[2]R&D Center for High Power Microwave Device, Institute of Electronics, Chinese Academy of Sciences, Beijing, China

Abstract—If sampling frequency is not high enough, the effect of adaptive memory polynomial predistortion linearizer is not very good for TWTA linearization. In order to keep the adaptive memory polynomial predistortion linearizer valid, usually the output power level of the TWTA must be reduced, which corresponds to a reduced efficiency of the TWTA. In this paper, we present a digital predistortion linearizer by combining LUT (Look-Up-Table) and memory-effect compensation technique, which may provide good linear performance with less reduction of the output power and relatively low sampling frequency. The results of simulations and experiments show that good linearity improvement can be reached for an X-band TWTA with this predistortion linearizer.

1. INTRODUCTION

The demand for higher data rates in communication systems has resulted in more complex digital modulation techniques which require linear power amplifiers (PAs) with high efficiency. When multiple signals are sent to a communication system, the PAs must operate at a reduced power level with reduced efficiency in order to keep its distortion at an acceptable level. As a solution to this efficiency-linearity dilemma, several analog techniques have been proposed in

the literature [1–6] for the linearization of the PAs. Due to complex circuitry, stability issues, and insufficient linearization, the analog correction is cumbersome. The digital predistortion (DPD) technique has also been proven to be a very effective linearization approach for the PAs [7–9] and widely used for the PAs linearization with the recent advances in digital signal processorsdigital-to-analog converters (DACs), and analog-to-digital converters (ADCs). Furthermore, DPD provides accuracy in synthesizing the predistortion function due to a software platform that makes it suitable for multi-standard environments [10]. Now the DPD technique usually adopts memory polynomial predistortion linearizer based on the indirect learning architecture [11, 12].

Traveling wave tube amplifier (TWTA) and solid state power amplifier (SSPA) both belong to the PAs. However, compared with SSPA, TWTA suffers from much more severe amplitude and phase distortions in the output power saturated region, and usually the adaptive memory polynomial predistortion linearizer is not very effective on the TWTA linearization. When applying a two-tone test to the TWTA, a large number of harmonics and intermodulation products are generated. Generally, C/3IM and C/5IM are about -27 dBc and -45 dBc as the SSPA nears saturation [13]. However, when the TWTA nears saturation, C/3IM and C/5IM are about -10 dBc and -15 dBc [14]. Thus, in the process of linearization, only the third-order intermodulation distortions are accounted for the SSPA, whereas the third- and fifth-order intermodulation distortions are accounted for the TWTA. So it is often assumed that a proper Nyquist sampling rate must be required for sampling such input and output waveforms to obtain truer TWTA distortion characteristics [15]. For a wideband input signal, the relatively low sampling frequency with the required resolution being 12 to 14 bits has a severe effect on TWTA linearization. But the relatively high sampling frequency with the required resolution being 12 to 14 bits results in significant challenges to realize cost-effective adaptive predistortion systems.

In this paper, the reason for above-mentioned phenomenon is analyzed, and then a digital predistortion linearizer is presented, designed, and realized by combining LUT (Look-Up-Table) and memory-effect compensation technique to get a good linear performance with relatively low sampling frequency and less reduction for the output power level of the TWTA operation.

2. EFFECT OF THE MEMORY POLYNOMIAL PREDIS-TORTION LINEARIZER ON THE TWTA LINEARITY PERFORMANCE

The indirect learning architecture [11, 12], adopted in the memory polynomial predistortion linearizer, is shown in Figure 1. If the memory polynomial predistortion linearizer is adopted to linearize the TWTA, there may be some problems. The PA and identification block in Figure 1 can be regarded as a system of adaptive inverse modeling, as shown in Figure 2. The adaptive inverse system is composed of a nonlinear model and an inverse model. The nonlinear model is composed of PA (TWTA), coupler and attenuator, and the inverse
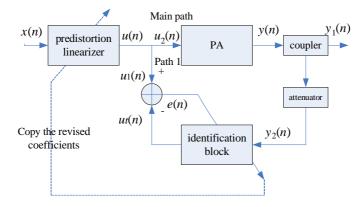

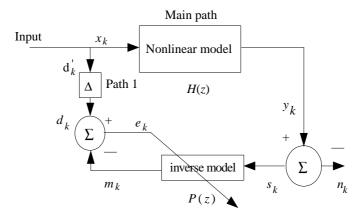**Figure 1.** Memory polynomial predistortion linearizer.

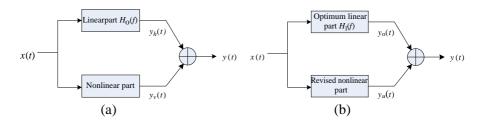**Figure 2.** Adaptive inverse system.

Figure 3. (a) Nonlinear model with parallel linear and nonlinear parts where their outputs may be correlative. (b) Nonlinear model with parallel-optimized linear and revised nonlinear parts where their outputs are not correlative.

model corresponds to identification block in Figure 1. The input signal is fed into a power splitter, and then divided into two equal components x_k and d'_k that pass through the main path and path 1, respectively. The output of nonlinear model is y_k. Fifth-order and other higher order intermodulation distortions, which are lost with the narrow sampling bandwidth, are defined as n_k. Then, $s_k = y_k - n_k$ and m_k are the input and output of the inverse model, respectively. In the adaptive inverse system, the signals x_k and s_k will be delayed as they go through a nonlinear model and inverse model, respectively. To obtain much lower value of minimum mean-square error, the delay (Δ samples) is included in path 1. d_k is the delayed signal.

In the adaptive inverse system, the nonlinear model is generally characterized by a single-input/single-output nonlinear model with parallel linear and nonlinear parts shown in Figure 3(a) [16]. The nonlinear part can be a general finite-memory part consisting of a zero-memory nonlinear part and a linear part. As shown in Figure 3(a), the total output $y(t)$ due to the input $x(t)$ is the sum of a linear output $y_h(t)$ and a nonlinear output $y_v(t)$. As a result, it is difficult to decompose the output auto-spectral $S_{yy}(f)$ into its linear and nonlinear components because the cross-spectrum term $S_{y_h y_v}(f) \neq 0$ [15]. A method, as shown in Figure 3(b) [16], can be used to solve the decomposition problems by changing this nonlinear model of Figure 3(a) so that $x(t)$ will give an optimum linear output $y_o(t)$ and an uncorrelated nonlinear output $y_u(t)$, i.e., the cross-spectrum term $S_{y_o y_u}(f) = 0$. And the input $x(t)$ is uncorrelated with the output $y_u(t)$, i.e., the cross-spectrum term $S_{xy_u}(f) = 0$. The output of optimum

linear and nonlinear part can be written as [16]

$$Y_o(f) = Y_h(f) + \left[\frac{S_{xy_v}(f)}{S_{xx}(f)} \right] X(f) \tag{1}$$

$$Y_u(f) = Y_v(f) - \left[\frac{S_{xy_v}(f)}{S_{xx}(f)} \right] X(f) \tag{2}$$

Referring to Figure 2, the transfer function of the nonlinear model is $H(z)$. As a result of the cross-spectrum term $S_{xy_u}(f) = 0$ in Figure 3(b), the third-order, fifth-order and other high order intermodulation distortions as the output of revised nonlinear system are uncorrelative with the input x_k. Thus, the input power spectrum can be given as [17]

$$\Phi_{ss}(z) = |H(z)|^2 \Phi_{xx}(z) - \Phi_{nn}(z), \quad z = e^{jw} \tag{3}$$

where $\Phi_{xx}(z)$ is the input power spectrum of the nonlinear model, $\Phi_{ss}(z)$ the input power spectrum of the inverse model, and $\Phi_{nn}(z)$ the power spectrum of the lost intermodulation distortions.

Because the delay does not alter the signal power, the cross spectrum $\Phi_{ds}(z)$ between the delayed signal d_k and the inverse model input s_k can be written as [17]

$$\Phi_{ds}(z) = G(z)\Phi_{dd}(z) = z^{\Delta} H(z)\Phi_{xx}(z) \tag{4}$$

where $G(z)$ is the transfer function from d to s, and z^{Δ} represents z-transform of the time delay.

When the mean-square error $MSE = \frac{1}{K} \sum\limits_{k=1}^{K} |e_k|^2$ (The amount of samples K is 1000, $e_k = d_k - m_k$) is minimized, the revised coefficients can be obtained. Then we can write the transfer function, composed of the revised coefficients, as [17]

$$P(z) = \frac{\Phi_{sd}(z)}{\Phi_{ss}(z)} = \frac{\Phi_{ds}^*(z)}{\Phi_{ss}(z)} = \frac{z^{-\Delta} H^*(z)\Phi_{xx}(z)}{|H(z)|^2 \Phi_{xx}(z) - \Phi_{nn}(z)} \tag{5}$$

If n_k is equal to zero, the auto-spectral $\Phi_{nn}(z) = 0$, so

$$P(z) = P_{opt}(z) = \frac{z^{-\Delta}}{H(z)} \tag{6}$$

Comparing Formula (5) with (6), only when $\Phi_{nn}(z)$ is zero, the result of Formula (5) approaches the optimal transfer function value. As the TWTA suffers from more and more severe amplitude and phase distortions in the output power saturated region, the amplitude of n_k will increase. Consequently, the increase of power spectrum $\Phi_{nn}(z)$ will make the result of Formula (5) far away from the optimal transfer function value.
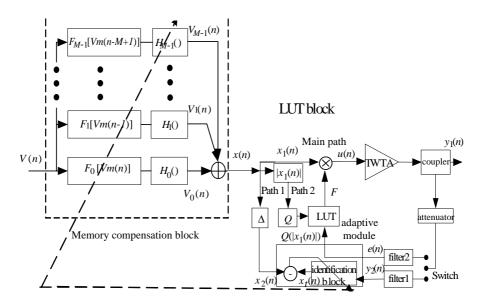
Figure 4. A new wideband digital predistortion linearizer.

3. A PROPOSED DPD FOR THE TWTA

Based on the above-mentioned discussions, a kind of wideband digital predistortion linearizer is proposed in this paper by combining LUT and memory-effect compensation technique for the TWTA, as shown in Figure 4. It is different from the memory polynomial predistortion linearizer. In the proposed DPD, two sampling paths are connected to the output of the TWTA with a switch, i.e., filter1 is used to select main signal and third-order intermodulation distortions, and filter2 for third- and fifth-order intermodulation distortions. The proposed DPD mainly consists of two blocks, i.e., memory compensation block and nonlinearity compensation block.

The memory compensation block of the proposed DPD consists of multiple branches connected in parallel. Each branch is composed of a nonlinear function $F_m(\cdot)$ and an impulse response $H_m(\cdot)$. These branches transform the input signal into a predistortion signal, which is combined with the instantaneous input signals, high-order input signals, and past input signals. The total predistorted signal is

expressed as [13]

$$x(n) = \sum_{m=0}^{M-1} V_m(n) = \sum_{m=0}^{M-1} H_m(F_m(V(n-m))) = \sum_{k=1}^{K}\sum_{m=0}^{M-1} b_{km}F_m(V(n-m))$$

$$= \sum_{k=1}^{K}\sum_{m=0}^{M-1} b_{km}V(n-m)|V(n-m)|^{k-1} \tag{7}$$

where $V(n)$ and $x(n)$ are the modulated signal and memory compensation signal, respectively. Here, b_{km} is the coefficient of the impulse response for different k and m. Parameter M specifies the number of the parallel branches, and K is the nonlinear order number of the proposed linearizer. Usually, the first order function of the impulse response $H_0(\cdot)$ is dominant, and the other components have small coefficient values. This digital predistortion linearizer can weaken memory effects using a simplified memory polynomial structure.

The nonlinearity compensation block is a LUT predistorter, as shown in Figure 4. The input signal $x(n)$ is fed into a power splitter, and then divided into three equal components that pass through the main path, path 1, and path 2, respectively. In the main path, the predistorted signal $u(n)$ is obtained by multiplying the input signal $x_1(n)$ and the corresponding predistortion complex gain F which is indexed in the LUT. The access of the LUT entries is given with the quantized signal from path 2, and the error signal from the adaptive module is used to determine how to update the LUT. In path 2, the corresponding amplitude of the main path signal $x_1(n)$ is quantized as $Q(|x_1(n)|)$ where the Q denotes a quantizer. The $Q(|x_1(n)|)$ is used as the access of the LUT entries to search the corresponding predistortion complex gain F. Simultaneously in path 1, the adaptive module is used to evaluate the LUT linearization performance with error signal. In the adaptive module, the way of extracting error signal in this paper is different from the memory polynomial predistortion linearizer. In memory polynomial predistortion linearizer, the error signal e_n of the amplifier is extracted from the main amplifier output end by subtracting the delayed signal $x_2(n)$. In the proposed DPD of this paper, the third- and fifth-order intermodulation distortions are chosen with filter2 as error signal e_n. If the error signal is greater than the rated value, the corresponding predistortion complex gain F will be updated with LMS (least mean square) algorithm [7] based on the error signal from the adaptive module.

After the LUT linearization for the TWTA, the amplitudes of the third-order, fifth-order, and other high order intermodulation distortions for the TWTA will decrease to a certain extent. Then we

can evaluate the TWTA linearization performance with the carrier-to-intermodulation (C/IM) ratio. According to this evaluation, the amount of memory compensation block coefficients can approximately be determined, which can reduce the complexity of the calculation. Thus, the highest nonlinear order number K is just 3, different from memory polynomial in the reference [12]. Memory compensation block coefficients can be updated using RLS (recursive least square) algorithm in the adaptive module with relatively low sampling frequency and less reduction for the output power level. The required error signal $e(n)$ for the RLS algorithm is extracted from $y_2(n)$ which is chosen with filter1 by subtracting the delayed signal $x_2(n)$, i.e., $e(n) = y_2(n) - x_2(n)$. The RLS algorithm process to solve for the memory compensation block coefficients b_{km} can be given as follows:

Step1: $B_k(0)$ and $P(0)$ are initialized as

$$B_k(0) = [0\ 0\ 0 \ldots 0\ 0]^T \tag{8}$$

$$P(0) = c^{-1}I \tag{9}$$

where c is a small and positive constant

$$\text{Step2}: K(n) = \frac{P(n-1)x_t(n)}{1 + x_t^T(n)P(n-1)x_t(n)} \tag{10}$$

$$\text{Step3}: e(n) = x_2(n) - x_t(n) \tag{11}$$

$$\text{Step4}: B(n) = B(n-1) - K(n)e(n) \tag{12}$$

$$\text{Step4}: P(n) = P(n-1) - K(n)x_t^T(n)P(n-1) \tag{13}$$

The estimation error $e(n)$ can be minimized by successive iteration from step2 to step5 so that the coefficients b_{km} can be updated. Finally, the revised coefficients of the identification block are copied to the memory compensation block.

In addition, one iteration process can only update one entry of the entire LUT, and it may take a long time before we update the entire LUT. To solve the problem, we apply the linear interpolation method [18] to the LUT. Linear interpolation formula can be written as follows

$$F(|x|) = \frac{|x_2| - |x|}{|x_2| - |x_1|}F(|x_1|) + \frac{|x| - |x_1|}{|x_2| - |x_1|}F(|x_2|) \tag{14}$$

where the amplitude of input signal $|x|$ is in the range of $(|x_1|, |x_2|)$.

On the premise of keeping the stability of the TWTA, the TWTA is respectively linearized by the LUT with and without the linear interpolation method. Then we evaluate the TWTA linearity performance by $NMSE = \frac{1}{N}\sum_{n=1}^{N}|e_n|^2$ (The number of samples, N,

is 1000, and e_n can be regarded as the error function between the nth output signal and corresponding ideal linear output signal), as shown in Table 1. Table 1 depicts NMSE for different LUT sizes with and without linear interpolation. To achieve high linearization requirement, the LUT size without the linear interpolation method must be large, so LUT will converge rather slowly, and the cost of the hardware will increase. The high linearization performance can be obtained by the linear interpolation method with reduced LUT size.

4. IMPLEMENTATION AND MEASUREMENT RESULTS

To validate the proposed DPD, we employ an 8.48-GHz orthogonal Frequency Division Multiplexing (OFDM) signal (10-MHz band and PAPR of 6 dB at CCDF = 0.01%). The Agilent's ADS (Advanced Design System) [19], Matlab, an ESG (electronic signal generator), a SA (spectrum analyzer) and a TWTA with an attenuator and filters are used for the test, as shown in Figure 5. And the photograph of this test system is shown in Figure 6. The correlative algorithm for the time-delay, LUT and RLS algorithm for the adaptive predistortion are programmed with Matlab code on PC. The linearization capability of the proposed DPD is evaluated using the practical TWTA by varying driving power level.

Table 1. LUT with and without the linear interpolation method.

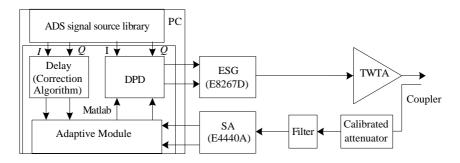| Size of LUT	64 (without linear interpolation method)	256 (without linear interpolation method)	64 (with linear interpolation method)
NMSE	−21.2 dB	−26.2 dB	−26.3 dB

Figure 5. Experimental setup for linearization test.

The OFDM signal was injected into an X-band TWTA (single-carrier saturated output power is 50 dBm) by varying driving power level. For all measurements in this paper, the adjacent channels were defined as two 10-MHz bands adjacent to the main frequency channel. If third- and fifth-order intermodulation distortions need to be included, the sampling bandwidth is usually at least 100 MHz. When the sampling bandwidth is 60 MHz, the ACPR performance versus average output power with the narrow sampling bandwidth is shown in Figure 7. At average output power 44 dBm, the spectral improvement of the ACPR is only 0.5 dB from the TWTA to the TWTA with the typical DPD in Figure 1. If the proposed DPD is adopted, the ACPR for the TWTA can be improved to about −45 dBc when the average output power is backed off to 43 dBm. However, in order to obtain a similar improvement only using memory polynomial predistortion linearizer, the average output power must be backed off to 41 dBm. If average output power is needed to back off to 43 dBm for the similar improvement, the sampling bandwidth must be greater than 100 MHz. Thus, if the proposed DPD is adopted, the improvement of about −45 dBc for the ACPR of the TWTA can be obtained with relatively low sampling frequency (60 MHz) and less reduction for the output power level.

The AM/AM and AM/PM conversion characteristics of the TWTA and that of the LTWTA were tested at the center frequency of 8.48 GHz, as shown in Figures 8 and 9. In Figures 8 with 9, the memoryless nonlinear characteristics and the scattering of the output signals caused by memory effects are both reduced.

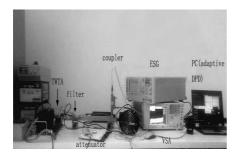Figure 10 shows the PSD of the OFDM signal with and without

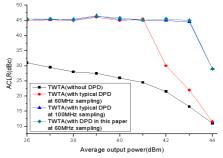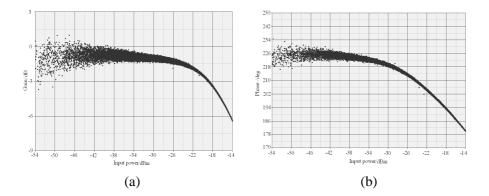**Figure 6.** Photograph of the test system.

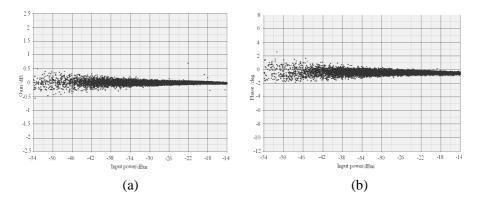**Figure 7.** TWTA ACPR comparison before and after linearization with narrow sampling bandwidth.

the proposed DPD at the output terminal of the TWTA with an average output power 43 dBm. When the LUT in the proposed DPD is updated, the ACPR can be improved to about −25 dBc. When the memory compensation block is used to follow the LUT, the ACPR can be improved to about −45 dBc. At this time, the PSD of the TWTA with the proposed DPD is only slightly different from the ideal PSD of the OFDM signal.

Figure 11 shows the learning curves of the proposed DPD discussed in the previous section. To obtain the NMSE, the errors, which are the differences between $V(n)$ and $y_2(n)$ in Figure 4, are

(a) (b)

Figure 8. Measured AM/AM and AM/PM before TWTA linearization. (a) AM/AM. (b) AM/PM.

(a) (b)

Figure 9. Measured AM/AM and AM/PM before TWTA linearization. (a) AM/AM. (b) AM/PM.
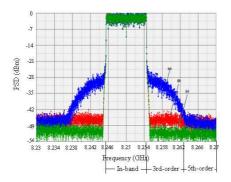
Figure 10. Measured TWTA OFDM spectra before and after linearization (a: LUT bmemory compensation c: ideal linear).
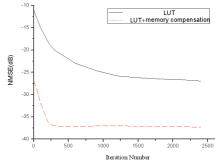

Figure 11. Learning curves versus number of iteration.

averaged over 200 independent trials. From the solid line in Figure 11, it can be seen that approximately 1500 data are required to reach the NMSE of -26 dB when LUT is adopted. These results show that the LUT technique is effective for improving the linear performance of the TWTA. However, it is not easy to obtain NMSE lower than -30 dB (35 dB) with the LUT. If the memory compensation is adopted following the LUT, there will be space for further improvement. The dashed line in Figure 11 shows the convergence behavior of the proposed DPD. It can be seen that a significantly lower NMSE can be achieved in the steady state with a low steady-state error.

5. CONCLUSION

A digital predistortion linearizer by combining LUT and memory-effect compensation technique is proposed, which can provide good linear performance with relatively low sampling frequency and less reduction for the output power level. When the 10-MHz band OFDM signal of 8.48-GHz was injected into an X-band TWTA with this proposed DPD, an ACPR improvement about -45 dBc can be reached when the output average power back off from 44 dBm to 43 dBm with the only 60 MHz sampling bandwidth. In order to obtain a similar improvement, the TWTA with a memory polynomial predistortion linearizer must be backed off from 44 dBm to lower power level 41 dBm. If less reduction for the output power level is needed for a similar improvement, the sampling bandwidth should be greater than 100 MHz.

REFERENCES

1. Kenington, P. B., *High-Linearity RF Amplifier Design,* Artech House, Boston, MA, 2000.

2. Eid, E. E., F. M. Ghannouchi, and F. Beauregard, "Optimal feedforward linearization system design," *Microwave Journal*, Vol. 38, No. 11, 78–86, 1995.

3. Young, Y. W. Y., Y. Jaehyok, Y. N. Joongjin, H. C. Jeong, and K. Bumman, "Feedforward amplifier for WCDMA base stations with a new adaptive control method," *IEEE MTT-S Int. Microw. Symp. Dig.*, Vol. 2, 769–772, Seattle, WA, Jun. 2002.

4. Kim, Y., Y. Yang, S. H. Kang, and B. Kim, "Linearization of 1.85 GHz amplifier using feedback predistortion loop," *IEEE MTT-S Int. Microw. Symp. Dig.*, Vol. 4, 1675–1678, Baltimore, MD, 1998.

5. Ezzeddine, A. K., H. A. Hung, and H. C. Huang, "An MMIC C-band FET feedback power amplifier," *IEEE Trans. Microw. Theory Tech.*, Vol. 38, No. 4, 350–357, 1990.

6. Morris, K. A. and J. P. McGeehan, "Gain and phase matching requirements of cubic predistortion systems," *Electron. Lett.*, Vol. 36, No. 21, 1822–1824, Oct. 2000.

7. Cavers, J. K., "Amplifier linearization using a digital predistorter with fast adaptation and low memory requirements," *IEEE Trans. Veh. Technol.*, Vol. 39, No. 4, 374–382, Nov. 1990.

8. Wright, A. S. and W. G. Durtler, "Experimental performance of an adaptive digital linearized power amplifier," *IEEE Trans. Veh. Technol.*, Vol. 41, No. 4, 395–400, Nov. 1992.

9. Ding, L., G. T. Zhou, D. R. Morgan, Z. Ma, S. Kenney, J. Kim, and C. R. Giardina, "A robust digital baseband predistorter constructed using memory polynomials," *IEEE Trans. Commun.*, Vol. 52, 159–164, Jan. 2004.

10. Kennington, P. B., "Linearized transmitters: An enabling technology for software defined radio," *IEEE Commun. Mag.*, Vol. 40, 156–162, Feb. 2002.

11. Li, J. and J. low, "A least-squares Volterra predistorter for compensation of non-linear effects with memory in OFDM transmitters," *Proc. of IEEE Communication Networks and Services Research Conference (CNSR)*, 197–202, Halifax, Canada, 2005.

12. Eun, C. and E. J. Powers, "A new Volterra Predistorter based on the indirect learning architecture," *IEEE Trans. Signal Processing*, Vol. 45, No. 1, 223–227, Jan. 1997.

13. Jangheon, K., Y. W. Young, M. Junghwan, and K. Bumman "A new wideband adaptive digital predistortion technique employing feedback linearization," *IEEE Transaction on Microwave Theory and Techniques*, Vol. 56, No. 2, 385–392, 2008.

14. Qiu, J. X., D. K. Abe, B. Levush, and B. G. Danly, "TWT performance enhancement using higher-order predistortion linearization techniques," *Military Communications Conference*, Vol. 5, 2830–2836, 2005.

15. Vaughan, R. G., N. L. Scott, and D. R. White, "The theory of Bandpass Sampling," *IEEE Trans. Signal Processing*, Vol. 39, No. 9, 1973–1991. Oct. 1991.

16. Julius, S. B., *Nonlinear System Analysis and Identification From Random Data,* 223, John Wiley and Sons, NY, 1990.

17. Widrow, B. and S. D. Stearns, *Adaptive Signal Processing,* 232–236, Prentice-Hall, New Jersey, 1985.

18. Abramowitz, M. and I. A. Stegun, *Handbook of Mathematical Functions,* 722, Dover Publications, New York, 1972.

19. Advanced Design System, Version 2002, Agilent Technologies, 41, USA.